CMS Draft Analysis Note

The content of this note is intended for CMS internal use and distribution only

2013/12/09
Head Id: 168171
Archive Id: 162946:168171MP
Archive Date: 2013/01/29
Archive Tag: trunk

Search for long-lived neutral particles decaying to photons

Giovanni Franzoni, Shih-Chuan Kao, Yuichi Kubota, Tambe Norbert, and Roger Rusack
University of Minnesota

Abstract

A search for long-lived neutral particle decaying into photons is performed using 19.1 fb^{-1} of proton-proton collision data at $\sqrt{(s)} = 8\,\text{TeV}$. We present a method which exploring its long-lived feature by using the time measurement from the ECAL. A data-driven method to predict anonymous sources of background is also developed. The method is sensitive to the lifetime ($c\tau$) beyond 1000 mm. Taking GMSB as target model and applying our method to data, no significant excess is observed. An upper limit at 95% C.L. is set.

1 Introduction

After the observation of the new neutral boson at the LHC, it indicates strong possibility for the existence of the Standard Model Higgs and encourages the search for the physics beyond the Standard Model. Since many theories suggest the format of long-lived particles, most possible candidate is neutralino ($\tilde{\chi_0}$) which decays into a photon and a weakly interacting stable gravitino ($\tilde{G}$) that is invisible for the CMS detector. Therefore, the photons and missing energy from event topology are the signature. In addition to excellent energy resolution, the fine granularity and great time resolution of CMS electromagnetic calorimeter (ECAL) become the useful applications to search long-lived neutral particles decaying to photons. In current scheme of the Standard Model, there is no direct physics process from TeV level proton-proton collisions showing the delayed timing. Therefore, the use of ECAL timing provides a great application to perform the search with nearly zero background. In this study, we explore the features of topological parameters of cluster shape and timing from ECAL and applied them to the search of long-lived neutral particle decaying to photons.

2 Data and Monte Carlo samples

The data used in the analysis was collected during 2012 runs with integrated luminosity of 19.1 fb^{-1}. The dataset is summarized in table 1. The Monte Carlo (MC) samples are generated by `PYTHIA 6`. The generation for signal samples adopt SUSY GMSB(Gauge-Mediated Supersymmetry Breaking) scheme where the free parameters, the SUSY breaking scale (Λ), and the $\tilde{\chi_0}$ lifetime ($c\tau$) are varied to cover an appropriate range of phase space. In this analysis, the Λ is fixed at 180 TeV and the $c\tau$ is varied from 250 mm to 6000 mm. For the background, there is no specific process which causes the real time delay from the collisions. Therefore, $\gamma+$ jets samples are just used for timing calibration and sanity check. The samples from Monte Carlo simulation are listed in table 2 and table 3.

Dataset Name	Recorded Luminosity [fb^{-1}]
`/Run2012B/SinglePhoton/EXODisplacedPhoton-PromptSkim-v3`	5.1
`/Run2012C/SinglePhoton/EXODisplacedPhoton-PromptSkim-v3`	6.9
`/Run2012D/SinglePhoton/EXODisplacedPhoton-PromptSkim-v3`	7.1

Table 1: The dataset name and corresponding integrated luminosity of the data used in the analysis

$c\tau$ (mm)	σ_{LO} (pb)	number of events
250	0.0145	50112
500	0.0145	50112
1000	0.0145	50112
2000	0.0145	50112
3000	0.0145	50112
4000	0.0145	46944
6000	0.0145	50112

Table 2: The signal GMSB MC samples used in this analysis

3 Event and Object Selection

Since photons decayed from long-lived neutral particle is the main signature from the signal, it not only implies that the distinguishable timing difference between signal and background

$\hat{p_T}$	σ_{LO} (pb)	number of events
$50 \sim 80$	3322.3	1995062
$80 \sim 120$	558.3	1992627
$120 \sim 170$	108.0	2000043
$170 \sim 300$	30.1	2000069
$300 \sim 470$	2.1	2000130
$470 \sim 800$	0.212	1975231

Table 3: The $\gamma+$ jets samples used in this analysis

but also suggests that the photon does not necessarily points to the CMS interaction point. Therefore, the ECAL cluster shape also can be used to distinguish signal and background. An earlier study already displayed the selection of off-point photon by using variables such as S_{major} or S_{minor} [1, 2]. In our study, we use S_{minor} to ensure the quality of photons and exclude anomalous ECAL spikes. Figure 1 shows that many backgrounds events with large or negative timing have small S_{minor} value. A cut on S_{minor} could helps to lower the rate and keep signal efficiency. The other variable, S_{major} is also applied in our background estimation that fake photons from beam halo muons shows exceptional large value at S_{major} (figure 2).

Another common feature for long-lived neutral particles is missing energy since gravitino ($\tilde{G}$) is undetectable for the CMS detector. A cut on $\not{E}_T$ is also useful to lower the rate from the standard model backgrounds like $\gamma+$ jets process and QCD events. In principle, the ECAL time of photons from $\gamma+$ jets events is around event time. However its large cross-section makes the tail of its time spectrum not completely negligible.

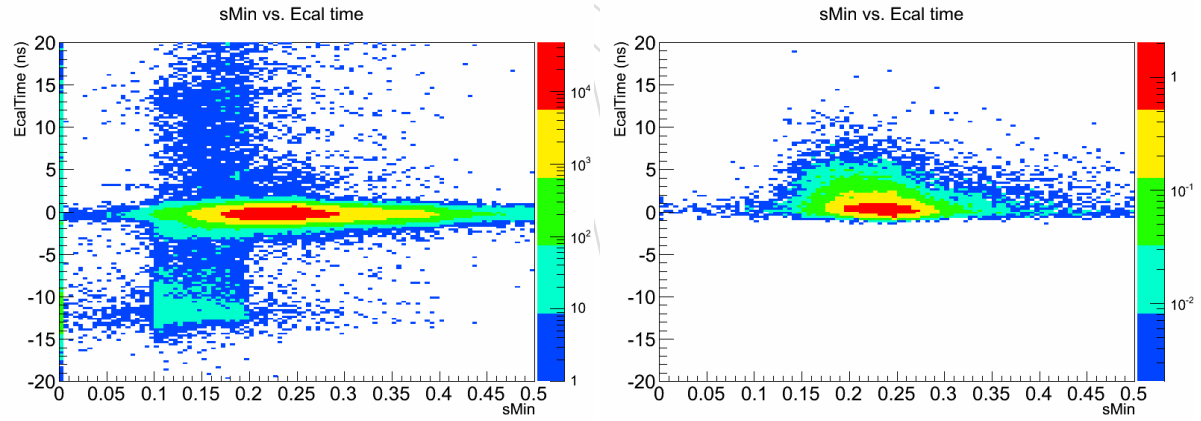

Figure 1: The S_{minor} v.s. ECAL time distribution for Data (left) and GMSB MC (right). The data sample has been pre-selected by HLT trigger

3.1 Trigger

The events are selected online using the trigger, HLT_DisplacedPhoton65_CaloIdVL_IsoL_PFMET25. The trigger was developed to devote displaced photon analysis. In order to avoid any model dependency, the trigger only require one isolated photon with p_T threshold 65 GeV and $\not{E}_T$ above 25 GeV. The efficiency and turn-on curve are studied separately since there are two objects in trigger definition. In order to decouple correlation between photon and E_T^{miss}, single muon dataset (HLT_IsoMu30) is used for efficiency measurement. The result is shown in Figure 3.

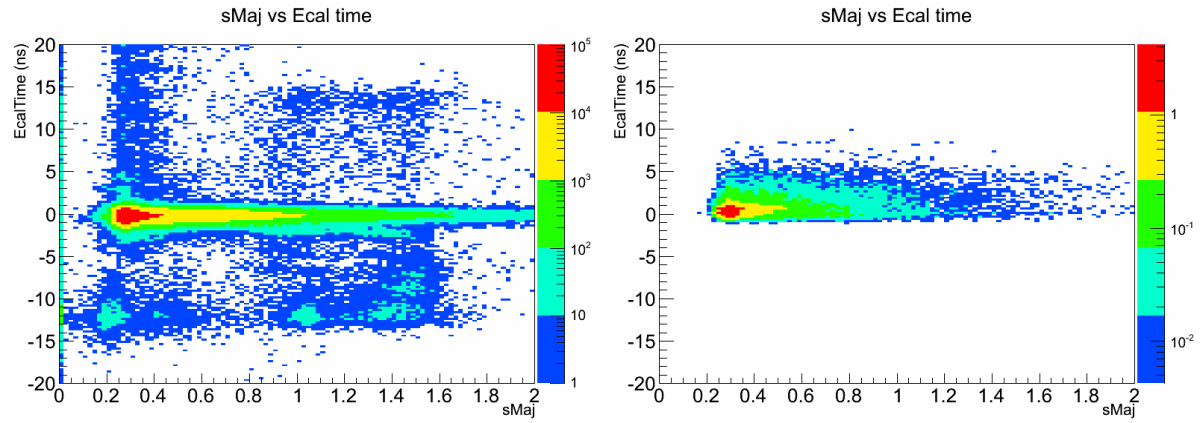

Figure 2: The S_{major} v.s. ECAL time distribution for Data (left) and GMSB MC (right). The data sample has been pre-selected by HLT trigger

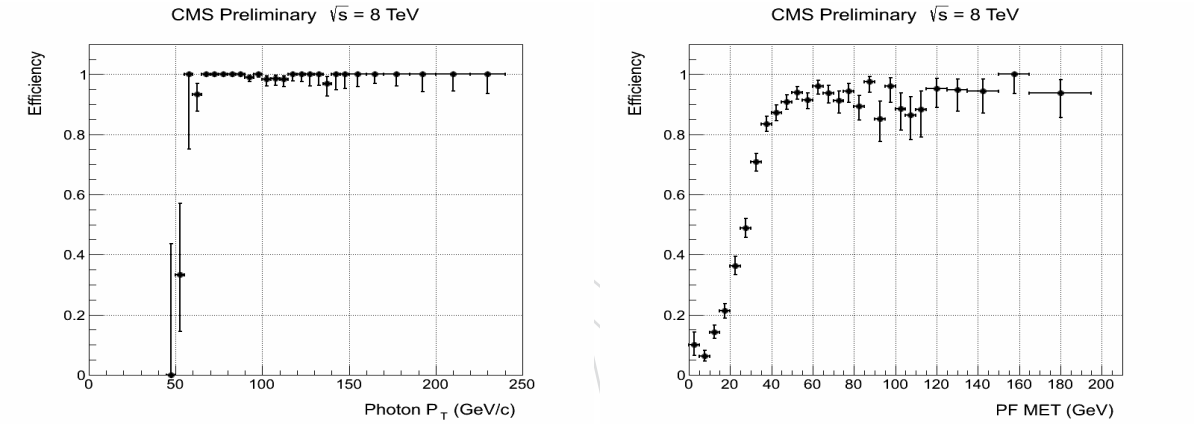

Figure 3: The trigger efficiency turn-on curve for the photon pT with $\not{E}_{\mathrm{T}} > 25$ GeV (left) and for $\not{E}_{\mathrm{T}}$ with photon $p_{\mathrm{T}} > 80$ (right)

3.2 Offline Event Selection

In order to have less model dependence, the offline selection has less dependence on jet multiplicity which relates to the final state of the event topology. The photon selection requires at least one photon in the event. The photon collection is extended to include "out-of-time" photons which are potential signal candidates.

The criteria for photon selection are listed below:

- The p_{T} of leading photon is greater than 80 GeV. Other photons in the event must have p_{T} greater than 45 GeV
- Photon from ECAL Barrel, i.e. —η— ¡ 1.47
- H/E < 0.05
- $\Delta R(track, photon)0.6$
- $0.12 \leq S_{minor} \leq 0.38$

For jets and $\not{E}_{\mathrm{T}}$ reconstruction, particle-flow algorithm is used which take tracking information into account for incomplete calorimeter measurement. Since neutralino decays to a photon and a gravitino, the missing energy is also a feature of event topology (figure 4). The $\not{E}_{\mathrm{T}}$ threshold is

set to 60 GeV due to the plateau of the efficiency from HLT PFMET25. The jet selection criteria are listed below.

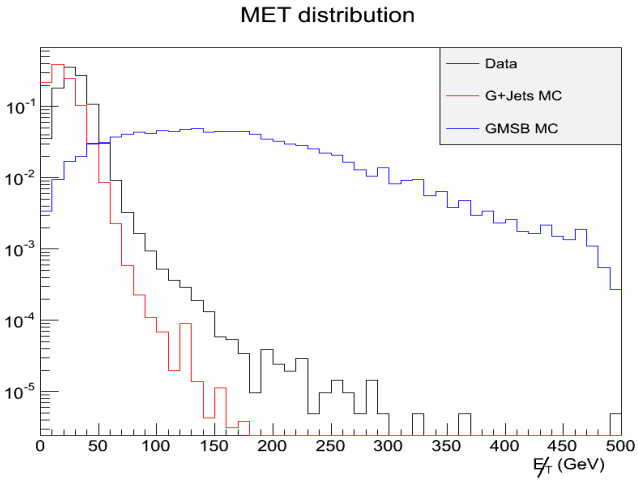

Figure 4: The $\not{E}_T$ distribution for data and MC samples

- Jet $p_T > 35$ GeV.
- Number of constituents > 1
- Charged EM energy fraction (CEF) < 0.99
- Neutral hadronic energy fraction (NHF) < 0.99
- Neutral EM energy fraction (NEF) < 0.99
- If $|\eta|$ of the jet < 2.4, charged hadronic energy fraction (CHF) > 0
- If $|\eta|$ of the jet < 2.4, charged multiplicity (NCH) > 0
- $\Delta R(jet, photon)0.3$

4 ECAL Time

The ECAL Time is the main observable from the signal in this study. The time measurement of ECAL crystal is determined from the raising edge of the pulse shape of the front-end electronics. We examed two different timing information in order to find out the most accurate way to retrieve timing information of the photon and reject the background, which are listed below.

- Seed time: Time form the seed crystal of the photon.
- Cluster time: The weighted averaged time from all the crystals in the seed basic cluster. A normalized χ^2 cut ($\chi^2 < 4$) is imposed.

The normalized χ^2 cut is computed among the crystals in the seed basic cluster. It is aim to reject the backgrounds which are the result of contamination form pile-up effect. (Figure 5). In this analysis, seed time is used as a current main observable but the normalized χ^2 is also applied to the photon object in order to remove possible fake photons.

The timing resolution is measured by the difference of the generated time and the reconstructed time from signal MC sample in three separated timing ranges (Figure 6). The study shows the resolution of ECAL timing measurement has consistent resolution across differet timing spectrum. The bias in large time zone (t > 5 ns) is observed but not significant since the major observation scope is beyond 2 ns in this study. The resolution between MC simulation and

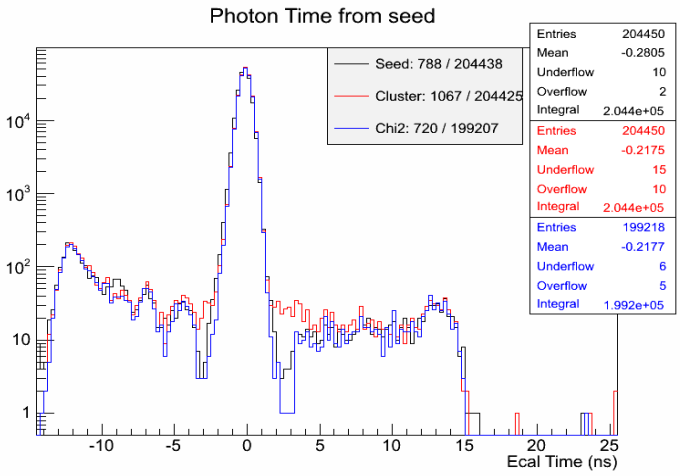

Figure 5: The timing distribution for inclusive single photon events

data is also studied by selecting events with only one or two jets. The $\gamma+$ jets MC samples are chosen. The result suggests that the central peak of timing from MC need to be shifted about 125 ps and additional smearing on resolution is also required (Figure 7).

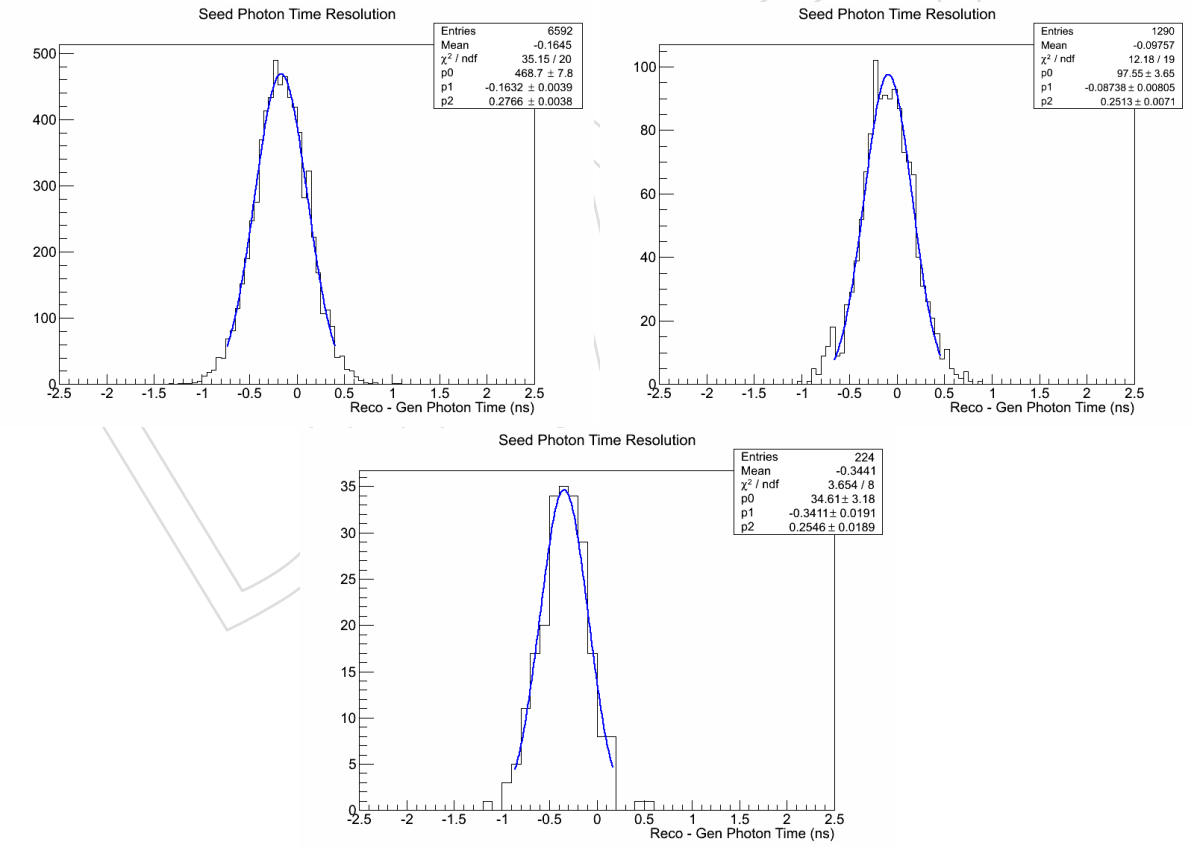

Figure 6: ECAL Time resolution in different timing range. Left (t $<$ 2 ns), middle (2 ns $< t <$ 5 ns), right (t $>$ 5 ns)

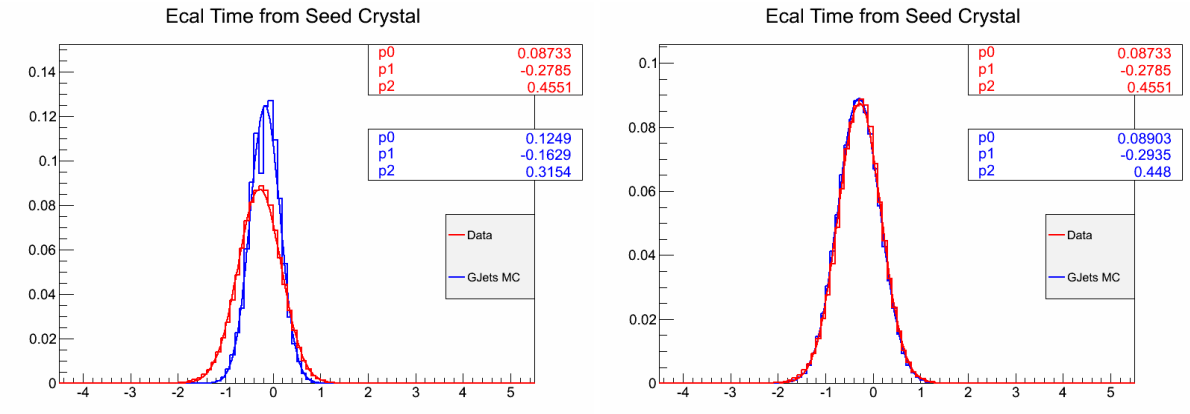

Figure 7: The comparison between time distribution between $\gamma+$ jets MC (blue) and Data (red) before (left) and after (right) calibration

5 Background Estimation

Since there is no timing constraint in event selection, the majority of events are from QCD $\gamma+$ jets process. Because their ECAL timing should be around the event time, its tail at large timing region is very negligible. Most significant sources for "out-of-time" photons are machine induced background (MIB), halo muons and anomalous ECAL spikes as well as cosmic-rays. The variables used in the background study are defined as below.

- CSC$\Delta\phi$, the ϕ difference between a CSC segment and a photon cluster.
- Number of good crystal, good crystal is defined as the crystal's ADC amplitude and noise ratio must smaller than 12.
- S_{Major} and S_{Minor}
- DT$\Delta\phi$ and DT$\Delta\eta$, the ϕ and η difference between a DT cosmic-ray segment and a photon cluster.

In order to study the background behavior, a nominal photon sample and a off-time photon sample are defined. The nominal photons have ECAL time between -1 ns and 1 ns and are from the events contain at least two jets. The off-timing photons are photons with ECAL time greater than 2 ns or smaller than -3 ns with no jet in the event. By comparing with these two samples, a summary of differences is listed belowed. Based on these phenomena, we classified background into three difference types, halo, spikes and cosmic-rays which are described in the following sections.

1. Clear matching between a CSC segment and their ECAL Cluster in off-timing sample (Figure 8).
2. Shape difference in number of good crystal of seed cluster of photons from two samples.
3. Different S_{Major} and S_{Minor} population (Figure 9).
4. Matching between a DT cosmic-ray segment and a photon cluster (Figure 10).

5.1 Halo Photon

Beam halo muons are known existing particles created by collsions of beam gas or scratching collimator from beams. While some of them hit and bremsstrahlung in the CMS ECAL detector

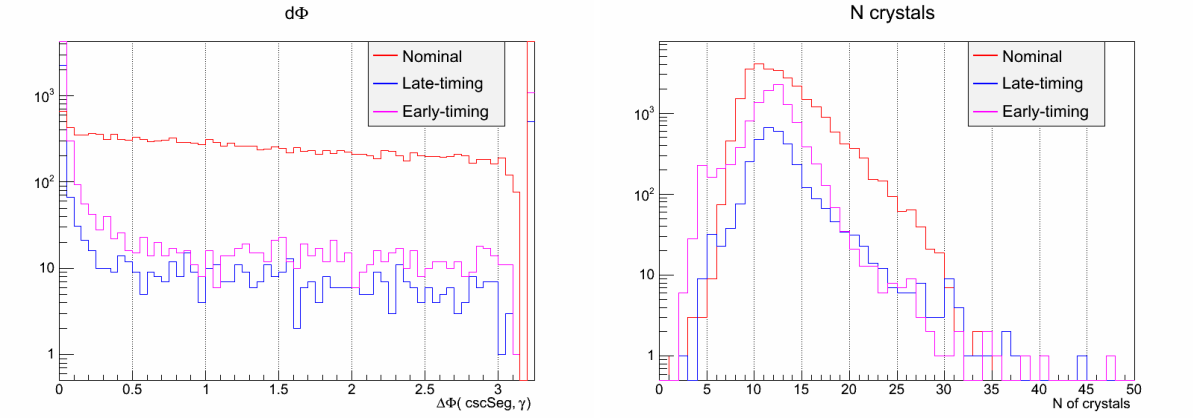

Figure 8: The comparison between nominal photon sample (red) and off-timing photon sample (blua) for CSC$\Delta\phi$(left) and number of good crystal(right)

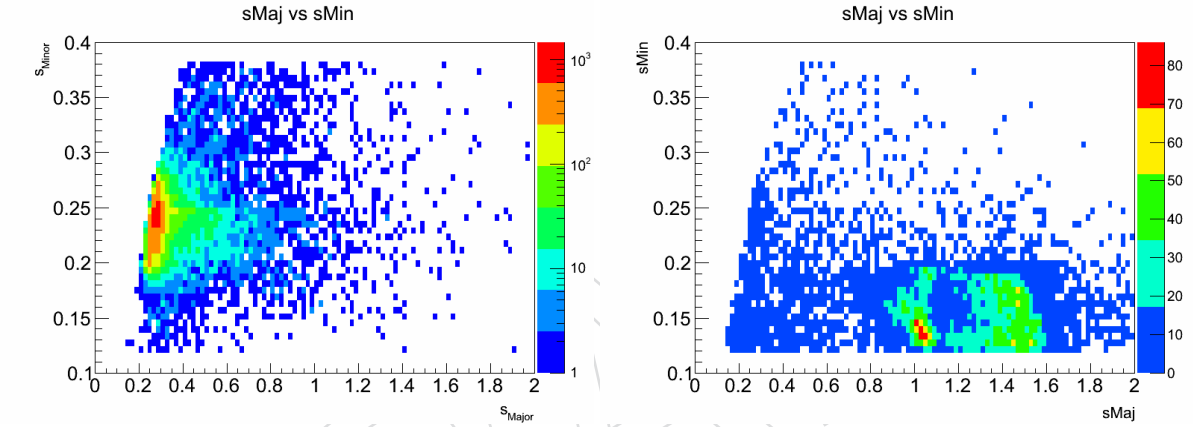

Figure 9: The comparison between nominal photon sample (left) and off-timing photon sample (right) for S_{Major} and S_{Minor}

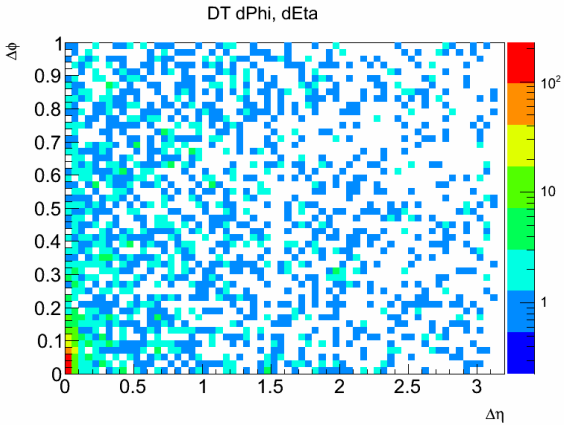

Figure 10: The DT$\Delta\phi\Delta\eta$ distribution from off-timing photon sample

which create photon like objects. Since they are created by halo muons, a possible muon track can be found in the Endcap muon system. Our study shows that a clear matching between a CSC segment and ECAL cluster is found. Additionly, the flying path of halo muons are

nearly parallel to the beam which result in a different, long ellipse shower shape which is corresponding to a larger S_{Major} and smaller S_{Minor}.

A simple estimation for the ECAL time from halo photons can be derived from

$$t_0 = \frac{r}{c} = \frac{\rho}{sin\theta}\frac{1}{c} \quad (1)$$

$$t_{halo} = \frac{z}{c} = \frac{\rho}{tan\theta}\frac{1}{c} \quad (2)$$

$$t_{ECAL} = t_{halo} - t_0 \quad (3)$$

$$= \frac{\rho}{c}(\frac{1}{tan\theta} - \frac{1}{sin\theta}) \quad (4)$$

$$= -\frac{\rho}{2c}tan(\theta/2) = -\frac{\rho}{2c}\exp^{-\eta} \quad (5)$$

where r is the distance between vertex and photon cluster, z is the z position of the photon cluster, c is the speed of light, θ is azimuthal angle. The reference time (t_0) is the function of η. This equation is under the assumption that halo muons travel parallel to the beam. Based on this estimation, a halo sample can be extracted by using this equation (Figure 11) and the pattern in η and ECAL time distribution at negative timing area can be understood. It also shows that most of halo are around ϕ about 0 or π.

Thus a subset of control sample for halo can be defined. By comparing with nominal sample, the azimuthal angle difference between a CSC segment and a photon cluster also show significant peak at $\Delta\,\phi < 0.05$.

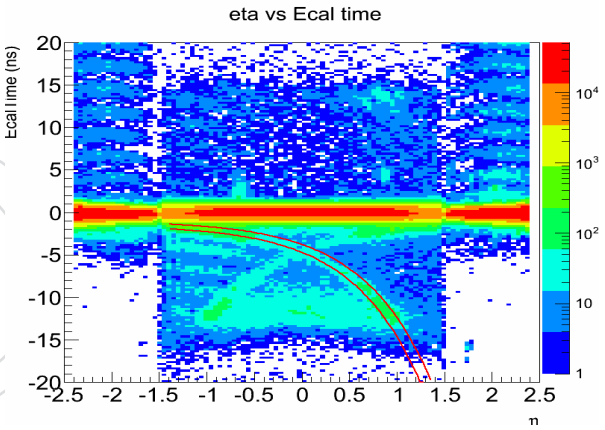

Figure 11: The η v.s. ECAL time for photons. The red curves show the fitting range to select halo control sample.

5.2 Cosmic-Ray

Similar to halo photons, cosmic-rays can possibily shower in the ECAL. Their existence can be found by looking at the $\Delta\phi$ and $\Delta\eta$ between a DT cosmic-ray muon segment and ECAL cluster. Due to the space between Muon Barrel system and ECAL, the actual DT positon used is projecting the position of DT segment to ECAL surface from its direction. A clear match at small $\Delta\phi$ and $\Delta\eta$ can be found (Figure 12).

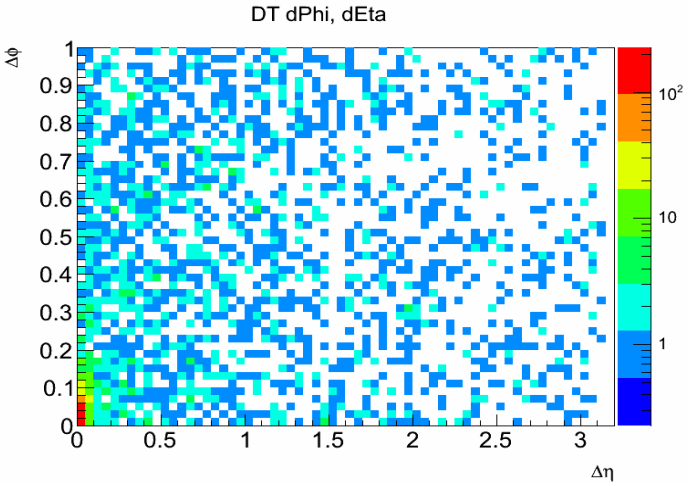

Figure 12: The $\Delta\eta$ and $\Delta\phi$ distribution for events with photon time greater than 2 ns or less than -3 ns

5.3 Anomalous ECAL Spike

ECAL spikes is known to be the energy deposit of Avalanche Photo-Diode (APD) from direct ionization of charged particles from collisions [3]. Although the topological "swiss-cross" method is implemented in the reconstruction process for removing them, some of them are still observed due to its high rate. This component can be addressed from the off-timing sample where no correlation is found from other detectors such as muon endcap or muon barrel system for halo and cosmic-ray muons. Due to its forming mechanism, its ECAL cluster size is expected to be smaller than the size of regular photons. After removing halo candidates from off-timing background control sample, a spike control sample display the feature that the number of good crystal in the seed basic cluster of the photon object is smaller than halo and nominal photon samples (Figure 13).

Based on their characters, the tagging criteria is defined below.

- Number of good crystal < 7
- $S_{Major} < 0.6$ and $S_{Minor} < 0.17$
- Not tagged as a halo and cosmic-ray photon

5.4 QCD and Pile-up

Due to 400 MHz RF frequency of the LHC, it provides 9 more LHC buckets for proton fills. The satellite bounches are thus formed by the causes of beam captured in incorrect locations at each stage of beam transfer between different machines. The existence of satellite bunches can be identified from their beam halo in the Endcap ECAL system of the CMS (Figure 14). A clear patten in 2.5 ns can be observed. Possible events from collisons between satellite bunches with late timing will be also the remaining source of our background. Unlike other background sources, it is the background from collisions. Therefore, no topological character can be applied to identify them for elimination. Since their kinematic feature would be similar, an ABCD method is then used for estimating the contamination in the signal region.

The ABCD regions are defined in different ECAL time zone and missing energy as shown in Figure 15. Since the early timing events and late timing events occur with the same reason and early timing region are signal free, the event ratio of low and high missing transverse energy

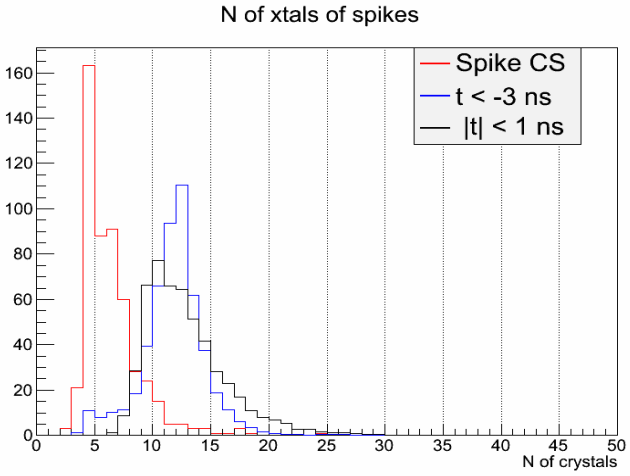

Figure 13: Number of crystal for photons for late timing region (t < -3 ns, blue histogram), control region ($|t|$ < 1ns, black) and spike control sample(red histogram). Three histograms are normalized to the sample amount.

will be propotional between early and late timing sample.

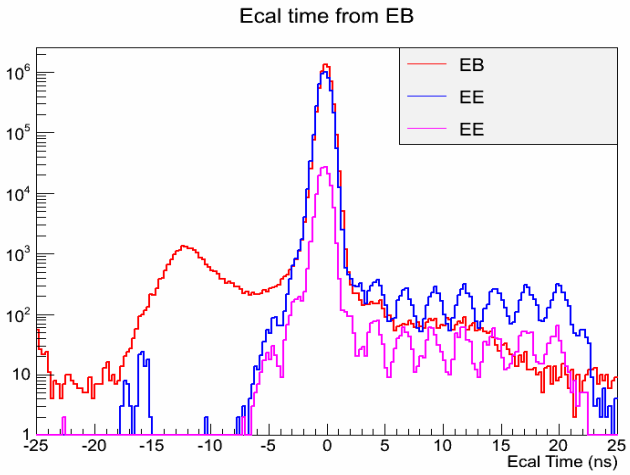

Figure 14: The ECAL timing from EB (red) and EE (blue). A clear 2.5 ns pattern can be found from EE timing due to halo from satellite bunches

5.5 Efficiency and Mis-tagging Rate

Based on the knowledge for various sources of background, we defined a halo control sample, halo and spike, which is used for studying its tagging efficiency and fake rate since it is the dominant contribution of background. The halo control sample is chosed by following requirments:

- 0-jet events
- Ecal Time < -3 ns
- $|\phi| < 0.1$ or $|\phi - \pi| < 0.1$
- $|\eta| < 1.45$
- Number of good crystal > 7

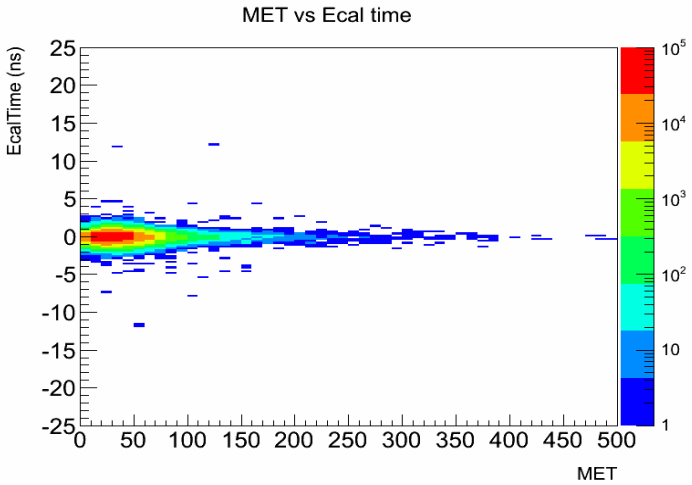

Figure 15: The ABCD plane for QCD backgrounds

And the halo tagging is defined as

- CSC$\Delta\phi < 0.05$
- $0.8 < S_{Major} < 1.65$ and $S_{Minor} < 0.2$

Thus the tagging efficiency is then measured from this control sample and mis-tagging rate can be determined from nominal sample (Figure 16). The mis-tagging rates for both sources are measured using the $\gamma+$ jets like events (at least two jet and $\not{E}_{\mathrm{T}} < 60$ GeV) with ECAL time $|t| < 1$ ns. According to the halo control sample, S_{major} shows the dependency with η (figure **??**). Thus the efficiency and mis-tagging rates for halo component are evaluated in 5 different $|\eta|$ slices from 0 to 1.4.

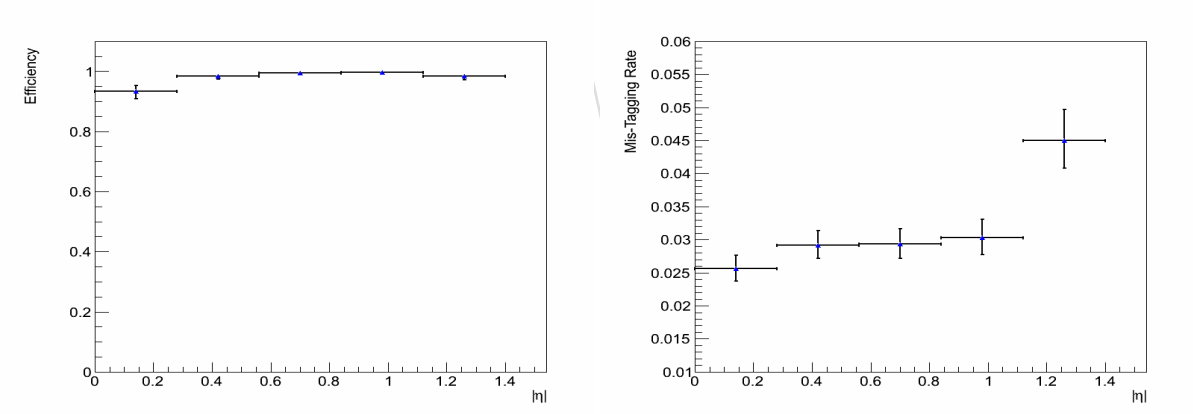

Figure 16: Tagging efficiency and mis-tagging rate for halo photons in 5 η regions

Since the tagging efficiency and mis-tagging rate are known, the portion for each component in the equation 6 can be solved by using following derivations,

$$B_1 = Q_1 + G_1 + H_1 \tag{6}$$
$$T(B_1) = tH_1 + mG_1 + mQ_1 \tag{7}$$
$$V(B_1) = vG_1 + nH_1 + nQ_1 \tag{8}$$

$$G_1 = \frac{nB_1 - V(B_1)}{n - v} \tag{9}$$

$$H_1 = \frac{mB_1 - T(B_1)}{m - t} \tag{10}$$

$$Q_1 = B_1 - G_1 - H_1 \tag{11}$$

where T and V are tagging operator for halo and spike respectively. t and v are the efficiency. m and n are the mis-tagging rate.

6 Systematic Uncertainties

The systematic uncertainties are taken into account of jet energy scale, jet energy resolution, $\not{E}_T$, egamma energy scale as well as photon timing resolution.

7 Result

The upper limit at 95 % C.L. is set (Figure 17).

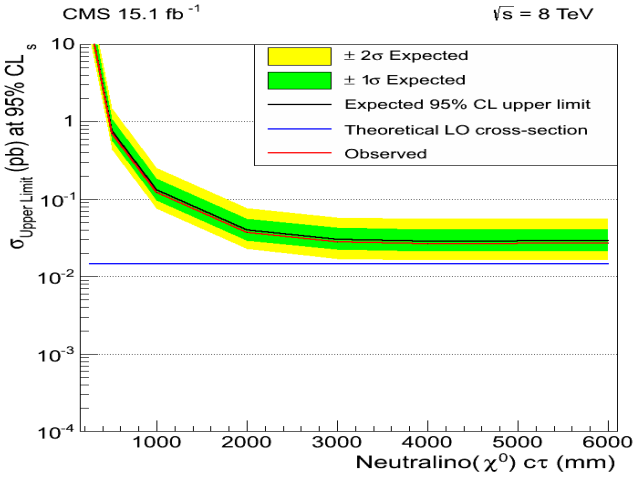

Figure 17: The upper limit at 95 % C.L. using CL_s method

8 References

References

[1] D. d. R. D. Franci, S. Rahatlou, "An algorithm for the determination of the flight path of long-lived particles decaying into photons", *AN-10-212* (2010).

[2] M. S. Daniele Del Re, Shahram Rahatlou and L. Soffi, "Search for Long-Lived Particles using Displaced Photons in pp Collisions at $\sqrt{s}$ = 7 TeV", *AN-11-081* (2012).

[3] CMS Collaboration, "Characterization and treatment of anomalous signals in the CMS Electromagnetic Calorimeter", *AN-10-357* (2011).